miR-532-3p inhibits the progression of tongue squamous cell carcinoma by targeting podoplanin

Zhi-Yun Liu, Chun-Guang Zhao

Department of Stomatology, The Sixth Hospital of Wuhan, Affiliated Hospital of Jianghan University, Wuhan, Hubei 430015, China.

Abstract

Background: The association between miR-532-3p and tongue squamous cell carcinoma (TSCC) has been examined in the literature to improve the survival rate of patients with this tumor. However, further studies are needed to confirm the regulatory roles of this microRNA (miRNA) in TSCC. The objective of this study was to investigate the roles played by and the underlying mechanism used by the miR-532-3p/podoplanin (*PDPN*) axis in TSCC development.

Methods: Western blotting and quantitative real-time reverse transcription-polymerase chain reaction (RT-qPCR) were performed to evaluate the *PDPN* expression level in TSCC tissues and cells. The proliferative, adhesive, and migratory capabilities of TSCC cells (CAL-27 and CTSC-3) were examined using cell counting kit-8 (CCK-8), cell adhesion, and wound-healing assays, respectively. The dual-luciferase reporter (DLR) assay was later conducted to confirm the relationship between miR-532-3p and *PDPN*.

Results: The results indicated that *PDPN* expression was enriched in TSCC tissues and cells, and that the expression of *PDPN* was associated with some clinicopathological parameters of TSCC, including lymph node metastasis ($P = 0.001$), tumor-node-metastasis (TNM) staging ($P = 0.010$), and grading ($P = 0.010$). Further analysis also showed that *PDPN* knockdown inhibited the viability, adhesive ability, and migratory capacity of CAL-27 and CTSC-3 cells, effects that could be reversed by the application of a miR-532-3p inhibitor. Additionally, *PDPN* was found to be a direct target of miR-532-3p.

Conclusions: This research suggested that by targeting *PDPN*, miR-532-3p could inhibit cell proliferation viability, adhesion, and migration in TSCC. Findings also revealed that the miR-532-3p/*PDPN* axis might provide more insights into the prognosis and treatment of TSCC.

Keywords: Tongue squamous cell carcinoma; Podoplanin; miR-532-3p

Introduction

Tongue squamous cell carcinoma (TSCC) is one of the tumors originating in the head and neck, and represents a substantial threat to human health owing to its high rate of recurrence and metastasis.[1-3] TSCC patients are often diagnosed at an advanced stage, thereby making clinical treatments more difficult.[4] Despite the use of treatment methods such as radiotherapy and chemoradiotherapy, the survival rate of patients with this tumor remains unsatisfactory.[5] Surgery has also proven not to be the best treatment option as it often results in unfavorable clinical outcomes and diminishes the quality of life of TSCC patients.[6,7] For these reasons, urgent research is needed to understand the molecular mechanism underlying the occurrence and development of TSCC.

The podoplanin (*PDPN*) gene plays an active role in the progression of many cancers. It is a protein-coding gene with high and specific expression in lymphatic endothelial cells, rendering it an effective lymphatic endothelium marker.[8,9] *PDPN* expression has been observed in various human cancers such as gastric carcinoma[10] and squamous non-small cell lung carcinoma.[11] In gastric carcinoma, high *PDPN* gene expression indicated poor overall survival and post-progression survival,[10] while in squamous non-small cell lung carcinoma, high levels of PDPN expression have been linked to poor clinicopathological features and prognosis.[11] In addition, *PDPN* has been demonstrated to influence the development of oral cancer.[12-17] However, little or no research has been performed to understand the impact of this gene on TSCC development.

Numerous microRNAs (miRNAs) are known to also influence the development of tumors. They are small, non-coding RNAs with roles in cellular metabolism, inflammation, and carcinomatosis.[18-20] Several abnormally expressed miRNAs have been identified in TSCC. For

Access this article online

Quick Response Code:

Website: www.cmj.org

DOI: 10.1097/CM9.0000000000001563

Correspondence to: Dr. Chun-Guang Zhao, Department of Stomatology, The Sixth Hospital of Wuhan, Affiliated Hospital of Jianghan University, No. 168 Hong Kong Road, Jianghan District, Wuhan, Hubei 430015, China
E-Mail: zhaochunguang18140@163.com

Chinese Medical Journal 2021;134(24)
Received: 22-09-2020 **Edited by:** Jing Ni

example, miR-488,[21] miR-409-3p,[22] and miR-23b[23] were reported to be significantly downregulated in TSCC, whereas miR-184[24] and miR-611[25] were reported to be upregulated. In one study, miR-532-3p was found to suppress TSCC progression by targeting CC-chemokine receptor 7 (CCR7).[26] However, no study has investigated the effect of miR-532-3p and *PDPN* on TSCC development.

Here, we investigated the role of *PDPN* and its relationship with miR-532-3p in the regulation of TSCC progression. The results of this research provide further insights into the multifaceted role of this miRNA in TSCC and reveal that the miR-532-3p/*PDPN* axis may be a novel therapeutic target for the treatment of TSCC.

Methods

Bioinformatics analysis

An mRNA expression profile GSE34105 from GEO DataSets (https://www.ncbi.nlm.nih.gov/gds/?term=) was used to screen the upregulated genes with log2FC (log2-fold change) >2 and adjusted $P < 0.05$. Then, the screened genes were uploaded to STRING (https://string-db.org/) for gene ontology (GO) analysis. To identify the upstream of *PDPN*, TargetScan (http://www.targetscan.org/vert_71/) and starBase (http://www.sysu.edu.cn) were used to predict the miRNAs binding to *PDPN*.

TSCC tissue samples

The tumor and adjacent normal tissues used in this study were collected from 27 patients with TSCC at the Sixth Hospital of Wuhan between September 2017 and June 2019. The tissue samples were frozen in liquid nitrogen immediately after they were collected from patients. Informed consent was obtained from the patients before the study, and this research was approved by the Ethics Committee of the Sixth Hospital of Wuhan (No. WHSHIRB-K-2019004). The clinical-stage was classified based on the 8th edition of the American Joint Committee on Cancer Tumor-Node-Metastasis (TNM) classification system.[27]. The association of gene expression with the clinicopathological features of TSCC cases are listed in Supplementary Table 1, http://links.lww.com/CM9/A933.

Cell culture and transfection

The human normal oral epithelial cell (HOEC) line was purchased from BeNa Culture Collection (BNCC, Beijing, China) and cultured in Dulbecco's modified Eagle's medium (DMEM) (Gibco, GrandIsland, NY, USA) supplemented with 10% foetal bovine serum (Hyclone, USA). The human TSCC cell lines CAL-27 and SCC-25 cell lines, both of which were purchased from Procell Life Science & Technology Co., Ltd (Wuhan, China), were kept in Gibco-provided DMEM and Gibco-provided DMEM/F12, respectively. Another TSCC cell line (CTSC-3) was obtained from ChemicalBook (Shanghai, China) and cultured in Roswell Park Memorial Institute (RMPI) 1640 Medium (Gibco). All the cell lines were cultured in their respective medium at 37°C in an atmosphere containing 5% CO_2. Cell transfection was conducted when the cell grown to 50% confluence using Lipofectamine 2000 Transfection Reagent (Thermo Fisher Scientific, San Jose, CA, USA). Small interfering RNA targeting *PDPN* (si-PDPN), the miR-532-3p mimic, the miR-532-3p inhibitor, and the negative control (NC) were purchased from RiboBio (Guangzhou, China), and were transfected at a concentration of 50 nmol/L. The transfected cells were collected after 48 h for further analyses.

RT-qPCR assessment

RNA was isolated from CAL-27 and CTSC-3 cells using the mirVana miRNA Isolation Kit (Thermo Fisher Scientific). RNA was then reverse-transcribed into complementary DNA (cDNA) using the one-step miRNA reverse transcription kit (HaiGene, China). qPCR was performed with the GoTaq qPCR Master Mix (Promega, Madison, WI, USA). For *PDPN*, total RNA was extracted from tissues and cells using the RNAeasy spin column-based Animal RNA Isolation Kit (Beyotime, Guangzhou, China). The extracted RNA was then reverse-transcribed using the BeyoRT II First Strand cDNA Synthesis Kit with gDNA Eraser (Beyotime). qPCR was then performed using the BeyoFast SYBR Green qPCR Mix (2 ×, High ROX) (Beyotime) in a Bio-Rad CFX96 Real-Time Detection instrument (Bio-Rad, Hercules, CA, USA). *GAPDH* and *U6* were used as reference genes, and the $2^{-\Delta\Delta Ct}$ method was used for quantification. The primer sequences for qPCR are listed in Supplementary Table 2, http://links.lww.com/CM9/A934.

Western blotting analysis

HOEC, CAL-27, CTSC-3, and SCC-25 cells were seeded in 6-well plates (2.5×10^5 cells/well) for transfection. After 48 h of transfection, the cells were lysed with pre-cooled radioimmunoprecipitation assay (RIPA) lysis buffer (Pierce, Rockford, IL, USA) containing protease inhibitors. Total protein (40 μg) was separated using 10% SDS–polyacrylamide gel electrophoresis (under 80 V for 20 min and then 100 V for 1 h). Subsequently, the protein was transferred to polyvinylidene fluoride (PVDF) membranes. After blocking with 5% skimmed milk, the membranes were incubated overnight at 4°C with primary antibodies against *PDPN* (1:1000, Cat#: AV44528, Merck, Rahway, NJ, USA) and β-actin (1:1000, Cat#: A1978, Merck). The next morning, the membranes were incubated with the secondary antibody (1:5000, Merck) for 1 h at 25°C. The bands were developed using the enhanced chemiluminescence (ECL) Plus Western Blotting Substrate (Thermo Fisher Scientific) and later analyzed using ImageJ software.

CCK-8 assay

Briefly, approximately 1000 cells/well were seeded into a 96-well plate and transfected when the cell grown to 50% confluence. Then, 10 μL/well of CCK-8 solution (Dojindo, Kumamoto, Japan) was added to the wells and incubated for 60 min. The absorbance of the wells was determined at 450 nm using a microplate reader (Bio Tek, Winooski, VT, USA). The plate was analyzed at intervals of 24 h for 3 days.

Cell adhesion assay

The cell adhesion assay was performed to explore the adhesive ability of CAL-27 and CTSC-3 cells. First, a

96-well plate was prepared by coating it overnight with fibronectin (Sigma-Aldrich, Louis, MO, USA) at 4°C, followed by blocking overnight at 4°C with 1% bovine serum albumin (BSA; Sigma-Aldrich). After that, 5×10^4 cells were suspended in serum-free medium, seeded in a 96-well plate, and incubated for 30 or 60 min. Non-adhering cells were washed off with PBS. Next, DMEM containing 10% foetal bovine serum was added to each well, and the mixture was incubated at 37°C for 4 h. A 10 μL aliquot of 3-(4, 5-Dimethylthiazol-2-yl)-2, 5-diphenyltetrazolium bromide (MTT) substrate was subsequently added to each well, and the mixture was incubated at 30°C for 2 h. The MTT-treated cells were then dissolved in 100 μL of dimethyl sulfoxide (DMSO). Finally, the absorbance was measured at 570 nm using a microplate reader (Bio Tek).

Wound-healing assay

A wound-healing assay was applied to detect the migratory capability of CAL-27 and CTSC-3 cells. Transfected cells (5×10^5 cells/well) were first seeded in a 6-well plate and cultured. Next, a scratch was made in the cells using a pipette tip (200 μL), the unattached cells were removed using PBS, and the wound width was observed and photographed under a microscope (Leica, Bensheim, Germany). After 24 h of incubation in serum-free medium, the wound width in each group was again photographed and recorded.

Dual-luciferase reporter assay

A dual-luciferase reporter (DLR) assay system (Promega) was used to confirm the direct interaction between miR-532-3p and *PDPN*. The wild-type (WT) or mutant (MUT) 3′UTR of *PDPN* (GeneScript, Nanjing, China) was subcloned into pMIR-REPORT Luciferase [Supplementary Digital Content, Figure 1, http://links.lww.com/CM9/A601] (Thermo Fisher Scientific) and then co-transfected with miR-532-3p mimic or miR-NC into CAL-27 and CTSC-3 cells. The transfected cells were seeded in the 96-well plate at a density of 1×10^4 cells/well and incubated for 48 h. The relative luciferase activity was detected in a microplate reader (Bio Tek).

Data analysis

Data analysis was conducted using SPSS 22.0 software (SPSS, Chicago, IL, USA). One-way analysis of variance (ANOVA) followed by Dunnett's *post hoc* test was employed for multiple comparisons, while a paired two-tailed *t* test was applied for comparisons between two groups. *P* values of < 0.05 were considered statistically significant. The association of miR-532-3p and *PDPN* expression with the clinicopathological features was analyzed by chi-square test or Fisher exact test. All the data were expressed as mean ± standard deviation. Each experiment was performed three times to minimize errors.

Results

PDPN is highly expressed in TSCC tissues and cells

The GEO dataset GSE34105 was used as the mRNA expression profile for identifying upregulated genes. Using a $\log_2$-fold change (FC) > 2 and an adjusted $P < 0.05$ as a cut-off, a total of 414 upregulated genes were identified and then uploaded to the STRING database (https://string-db.org/) for further gene ontology (GO) analysis. As shown in Figure 1A, we identified five genes (*CXCL13*, *CCL19*, *CCL5*, *PDPN*, and *PTPRC*) that were associated with cell adhesion, cell proliferation, and cell migration. After reviewing the literature, *PDPN* was selected as the gene of interest because of its high expression and reported promotive functions in oral cancer.[15,16] RT-qPCR and Western blotting were used to characterize the expression of *PDPN* in TSCC. As illustrated in Figure 1B, *PDPN* expression was higher in TSCC tissues (3.95 ± 1.94) than that in non-TSCC tissues (1.00 ± 0.34; $P < 0.001$). We subsequently divided the clinical samples into low and high *PDPN* expression groups based on the mean of the *PDPN* expression in TSCC tissues and then analyzed the correlation between *PDPN* expression and the clinicopathological features of TSCC. As shown in Supplementary Table 1, http://links.lww.com/CM9/A933, the expression of *PDPN* was associated with several clinicopathological features of TSCC, including lymph node metastasis ($P = 0.001$), TNM staging ($P = 0.010$), and grading ($P = 0.010$). However, the expression of *PDPN* was not significantly associated with gender ($P = 0.343$), age ($P = 0.883$), differentiation ($P = 0.153$), or tumor localization ($P = 0.354$). Compared with that in HOEC cells (1.00 ± 0.07), *PDPN* mRNA levels were significantly increased in CAL-27 (4.04 ± 0.08; $P < 0.001$), CTSC-3 (4.47 ± 0.14; $P < 0.001$), and SCC-25 cells (3.70 ± 0.12; $P < 0.001$) [Figure 1C]. Next, we assessed the change in the *PDPN* protein expression level, and found that it was increased in CAL-27 (1.86 ± 0.03; $P < 0.001$), CTSC-3 (1.99 ± 0.05; $P < 0.001$), and SCC-25 cells (1.61 ± 0.03; $P < 0.001$) compared with that in HOEC cells (1.000 ± 0.010) [Figure 1D].

PDPN was downregulated by si-PDPN

Given that *PDPN* might be involved in the regulation of TSCC, we used siRNA to knock down *PDPN* expression in CAL-27 and CTSC-3 cells. The RT-qPCR results showed that, following the transfection of si-PDPN, *PDPN* expression was decreased by about 70% in CAL-27 cells (0.22 ± 0.02 *vs.* 1.00 ± 0.05; $P < 0.001$) and by about 60% in CTSC-3 cells (0.31 ± 0.01 *vs.* 1.01 ± 0.06; $P < 0.001$) when compared with that in cells transfected with the blank control [Figure 2A]. Similarly, compared with the blank control group, the protein expression of *PDPN* was also reduced in si-PDPN-transfected CAL-27 cells (0.64 ± 0.04 *vs.* 1.00 ± 0.02; $P < 0.001$) and si-PDPN-transfected CTSC-3 cells (0.74 ± 0.06 *vs.* 1.00 ± 0.02; $P < 0.001$) [Figure 2B]. Overall, these results demonstrated that *PDPN* was downregulated by si-PDPN.

PDPN knockdown suppressed TSCC development

Next, we observed the effect of *PDPN* on TSCC development by assessing the proliferative, adhesive, and migratory capability of TSCC cells transfected with si-*PDPN*. The results of the CCK-8 assay showed that after a transfection period of 72 h, *PDPN* knockdown impaired the viability of CAL-27 (0.85 ± 0.05; $P < 0.001$) and

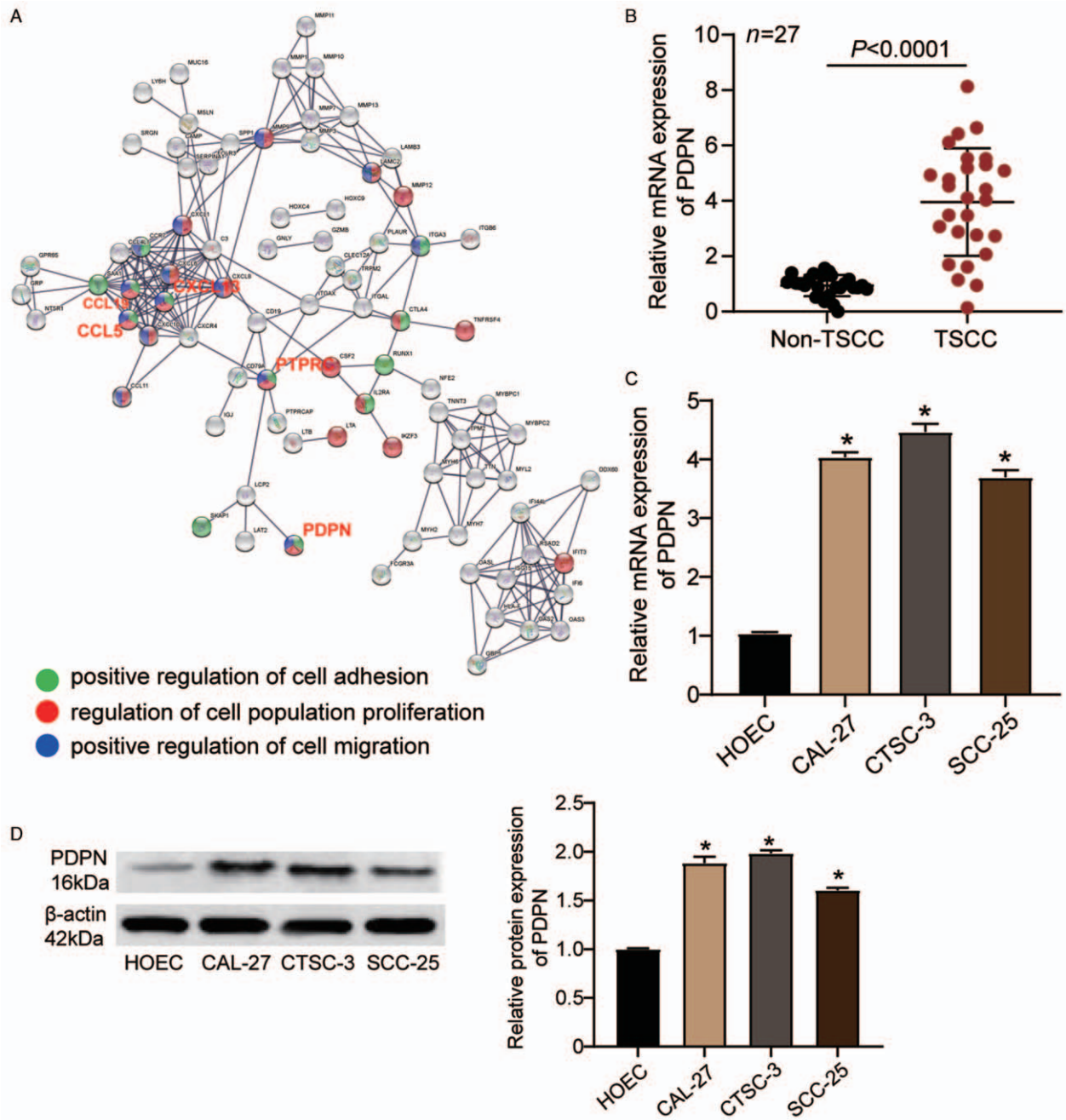

Figure 1: *PDPN* expression was increased in TSCC tissues and cells. (A) *CXCL13*, *CCL19*, *CCL5*, *PTPRC*, and *PDPN* were screened out, and are associated with cell adhesion, cell proliferation, and cell migration. (B) The mRNA expression of *PDPN* in TSCC tissues and corresponding non-TSCC tissues as determined by RT-qPCR. (C) The mRNA expression of *PDPN* in the HOEC and TSCC cell lines (CAL-27, CTSC-3, and SCC-25) as determined by RT-qPCR. (D) The protein expression of *PDPN* in the HOEC and TSCC cell lines (CAL-27, CTSC-3, and SCC-25) as determined by Western blotting. $^{*}P < 0.001$ *vs.* HOEC cells. HOEC: Human normal oral epithelial cell; *PDPN*: Podoplanin; RT-qPCR: Quantitative real-time reverse transcription-polymerase chain reaction; TSCC: Tongue squamous cell carcinoma.

CTSC-3 cells (1.02 ± 0.07; $P < 0.001$) compared with that in the blank control group (2.07 ± 0.05 and 2.13 ± 0.04, respectively) [Figure 3A]. A cell adhesion assay demonstrated that the adhesive capacity of si-PDPN-transfected CAL-27 cells was decreased at 60 min compared with that in cells transfected with the blank control ($60.60 \pm 2.79\%$ *vs.* $100.00 \pm 3.97\%$; $P < 0.001$), and a similar result was observed for CTSC-3 cells ($70.10 \pm 4.54\%$ *vs.* $100.00 \pm 2.52\%$; $P < 0.001$) [Figure 3B]. The wound-healing assay results showed that, compared with the blank control group, si-PDPN reduced the migratory ability of CAL-27 and CTSC-3 cells by about 40% (respectively $46.50 \pm 1.18\%$ *vs.* $77.70 \pm 4.24\%$; $P < 0.001$ and $39.50 \pm 2.14\%$ *vs.* $72.20 \pm 3.75\%$; $P < 0.001$) [Figure 3C]. Taken together, the results revealed that the knockdown of *PDPN* by si-PDPN could suppress TSCC development.

miR-532-3p targeted PDPN in TSCC cells

TargetScan and starBase were applied to identify which miRNAs bind to *PDPN*. The results showed 10 overlapping miRNAs between TargetScan and starBase

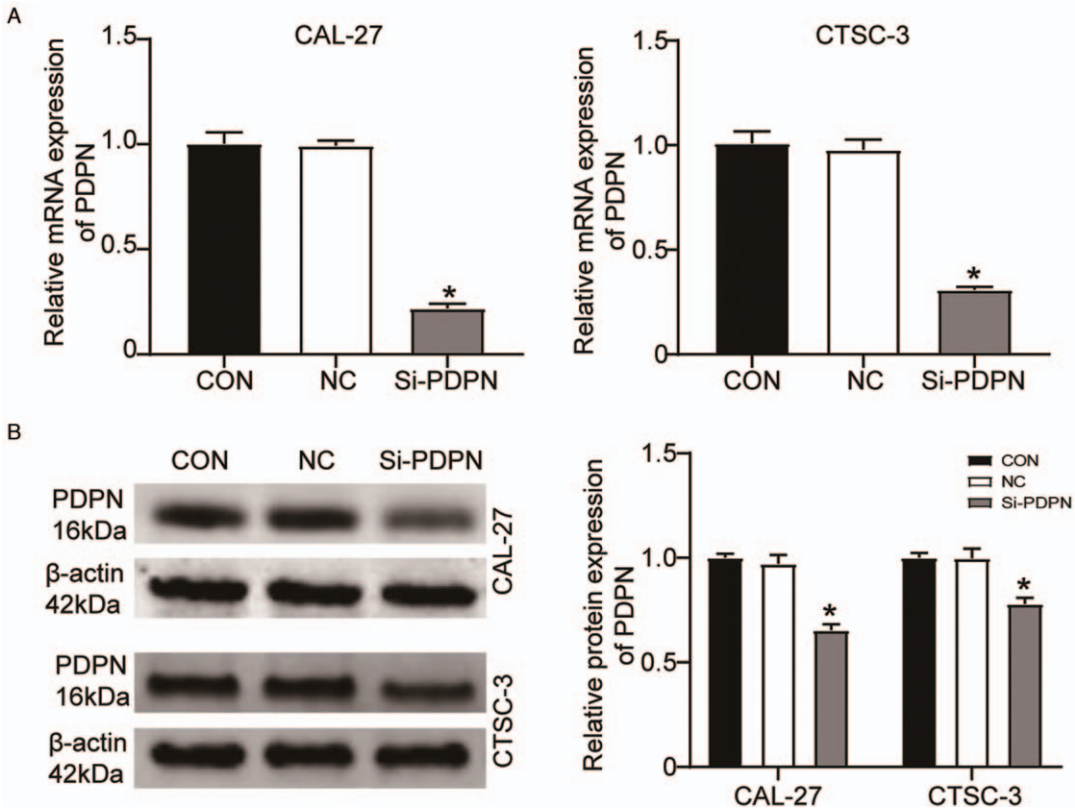

Figure 2: *PDPN* was downregulated by si-PDPN. (A) The mRNA expression of *PDPN* in CAL-27 and CTSC-3 cells after the transfection of si-PDPN as determined by RT-qPCR. (B) The protein expression of *PDPN* in CAL-27 and CTSC-3 cells after transfection of si-PDPN as determined by Western blotting. CON: Blank control group; NC: Negative control; *PDPN*: Podoplanin; RT-qPCR: Quantitative real-time reverse transcription-polymerase chain reaction. $^{*}P < 0.001$ *vs.* the blank control group.

[Figure 4A]. Among them, miR-532-3p attracted our attention because it had the highest score in TargetScan. The binding sites for miR-532-3p on the *PDPN* 3′UTR are shown in Figure 4B. The predicted relationship between miR-532-3p and *PDPN* was further determined through a luciferase reporter assay. As depicted in Figure 4C, luciferase activity decreased in CAL-27 and CTSC-3 cells co-transfected with the miR-532-3p mimic and WT of *PDPN* (PDPN-WT) (0.37 ± 0.05; $P < 0.001$ and 0.45 ± 0.02; $P < 0.001$, respectively) compared with that in CAL-27 and CTSC-3 cells co-transfected with the NC and PDPN-WT (1.00 ± 0.02 and 1.00 ± 0.02, respectively). This indicated that miR-532-3p could bind to the *PDPN* 3′UTR. Next, we characterized the changes in miR-532-3p expression in TSCC progression. As illustrated in Figure 4D, miR-532-3p expression was significantly reduced in TSCC tissues when compared with that in non-TSCC tissues (0.36 ± 0.13 *vs.* 1.00 ± 0.43; $P < 0.001$). We further found that there was a negative correlation between miR-532-3p and *PDPN* in TSCC tissue ($R^2 = 0.66$; $P < 0.001$) [Figure 4E]. Subsequently, we divided the clinical samples into low and high miR-532-3p expression groups based on the mean miR-532-3p expression in TSCC tissues and assessed whether there was a correlation between miR-532-3p expression and the clinicopathological features of TSCC. The result showed that the expression of miR-532-3p was significantly associated with lymph node metastasis ($P = 0.025$), TNM staging ($P = 0.004$), and grading ($P = 0.001$), but not with gender ($P = 0.863$), age ($P = 0.148$), differentiation ($P = 0.405$), or tumor localization ($P = 0.441$) [Supplementary Table 1, http://links.lww.com/CM9/A933]. Besides, compared with HOEC cells (1.00 ± 0.12), the levels of miR-532-3p were significantly reduced in CAL-27 (0.28 ± 0.03; $P < 0.001$), CTSC-3 (0.17 ± 0.02; $P < 0.001$), and SCC-25 cells (0.35 ± 0.04; $P < 0.001$) [Figure 4F]. The transfection efficiency of miR-532-3p is depicted in Figure 4G. Compared with the CON group (1.00 ± 0.05 in CAL-27 cells and 1.00 ± 0.04 in CTSC-3 cells), the expression level of miR-532-3p was decreased in the inhibitor-treated cells (0.29 ± 0.03; $P < 0.001$ in CAL-27 cells and 0.38 ± 0.01; $P < 0.001$ in CTSC-3 cells), but increased in those treated with the miR-532-3p mimic (3.41 ± 0.30; $P < 0.001$ in CAL-27 cells, and 3.03 ± 0.35; $P < 0.001$ in CTSC-3 cells). *PDPN* protein expression was also detected using Western blotting. The result revealed that *PDPN* expression was significantly enhanced by the miR-532-3p inhibitor in CAL-27 and CTSC-3 cells (1.86 ± 0.07; $P < 0.001$ and 1.77 ± 0.06; $P < 0.001$, respectively) compared with that in the blank control group (1.00 ± 0.02 and 1.00 ± 0.06, respectively), while it was reduced by the miR-532-3p mimic in CAL-27 and CTSC-3 cells (0.21 ± 0.03; $P < 0.001$ and 0.76 ± 0.02; $P < 0.001$, respectively) [Figure 4H].

miR-532-3p inhibitor treatment reversed the tumor inhibitory effect of PDPN knockdown

Rescue experiments were designed to understand the interaction between miR-532-3p and *PDPN* in TSCC cells. CCK-8, cell adhesion, and wound-healing assays were

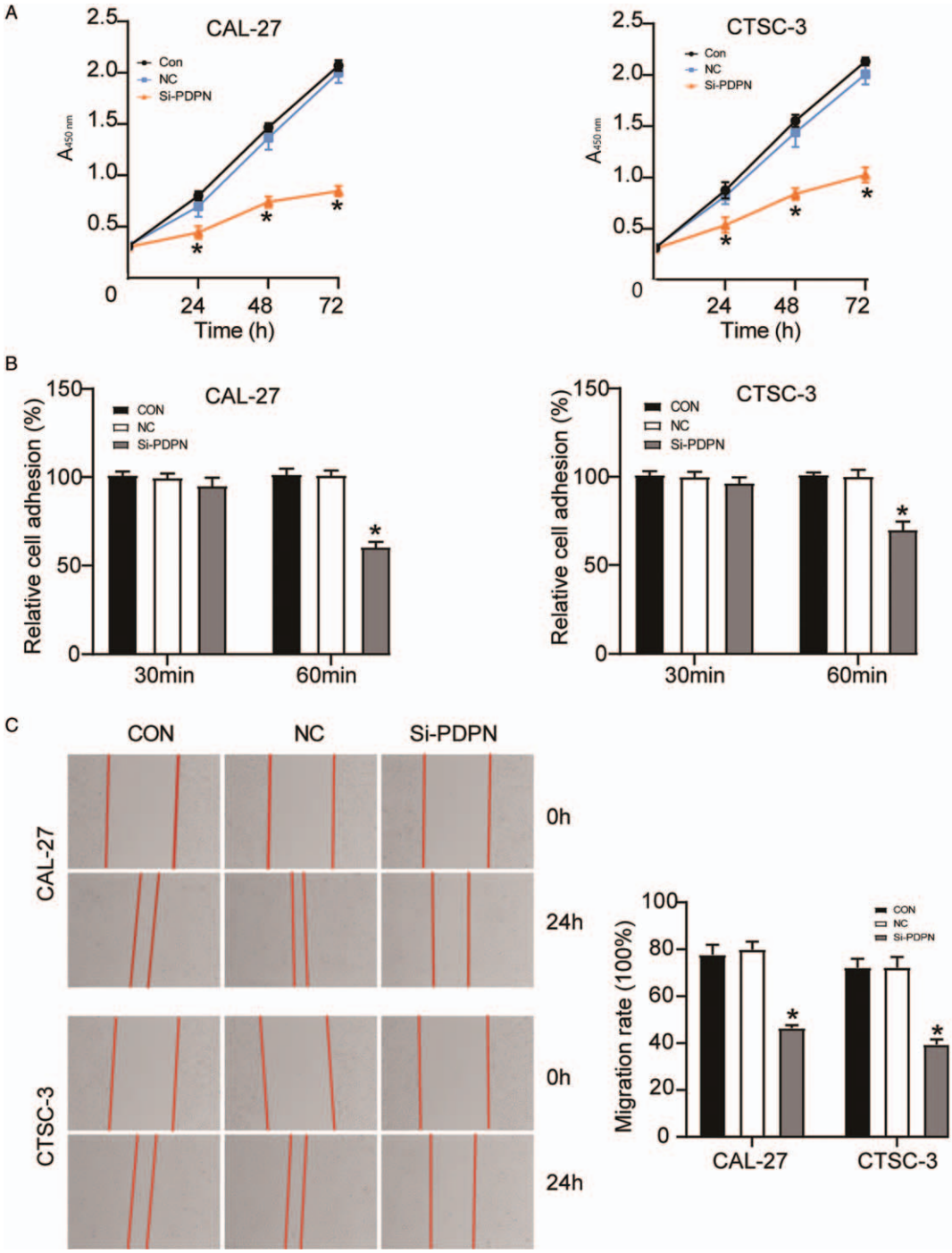

Figure 3: The knockdown of *PDPN* suppressed TSCC development. The cells were transfected with si-PDPN. (A): A CCK-8 assay was performed to assess the viability of CAL-27 and CTSC-3 cells. (B) A cell adhesion assay was performed to evaluate the adhesive ability of CAL-27 and CTSC-3 cells. (C): A wound-healing assay was performed to detect the migratory ability of CAL-27 and CTSC-3 cells. CCK-8: Cell counting kit-8; CON: Blank control group; NC: Negative control; OD: Optical density; *PDPN*: Podoplanin; TSCC: Tongue squamous cell carcinoma. $^{*}P < 0.001$ *vs.* the blank control group.

carried out to examine CAL-27 and CTSC-3 cells treated with si-PDPN or si-PDPN plus the miR-532-3p inhibitor. The CCK-8 assay result indicated that cell viability was increased in the si-PDPN + miR-532-3p inhibitor group (1.78 ± 0.07; $P < 0.001$ in CAL-27 cells and 1.91 ± 0.08; $P < 0.001$ in CTSC-3 cells) compared with that in the si-PDPN only group (1.02 ± 0.07 in CAL-27 cells and 1.13 ± 0.06 in CTSC-3 cells) after 72 h of transfection [Figure 5A]. The results of the cell adhesion assay showed that when si-PDPN was co-transfected with the miR-532-3p inhibitor, the inhibitory effect of si-PDPN on cell adhesion could be reversed ($81.30 \pm 2.21\%$ *vs.* $61.36 \pm 3.33\%$; $P < 0.001$ in CAL-27 cells and $88.10 \pm 3.80\%$ *vs.* $72.23 \pm 1.78\%$; $P < 0.001$ in CTSC-3 cells) [Figure 5B]. Similarly, the wound-healing assay result demonstrated that in CAL-27 and CTSC-3 cells, the level of cell migration in the si-PDPN + miR-532-3p inhibitor group ($70.60 \pm 2.13\%$; $P < 0.001$ and $61.30 \pm 4.29\%$;

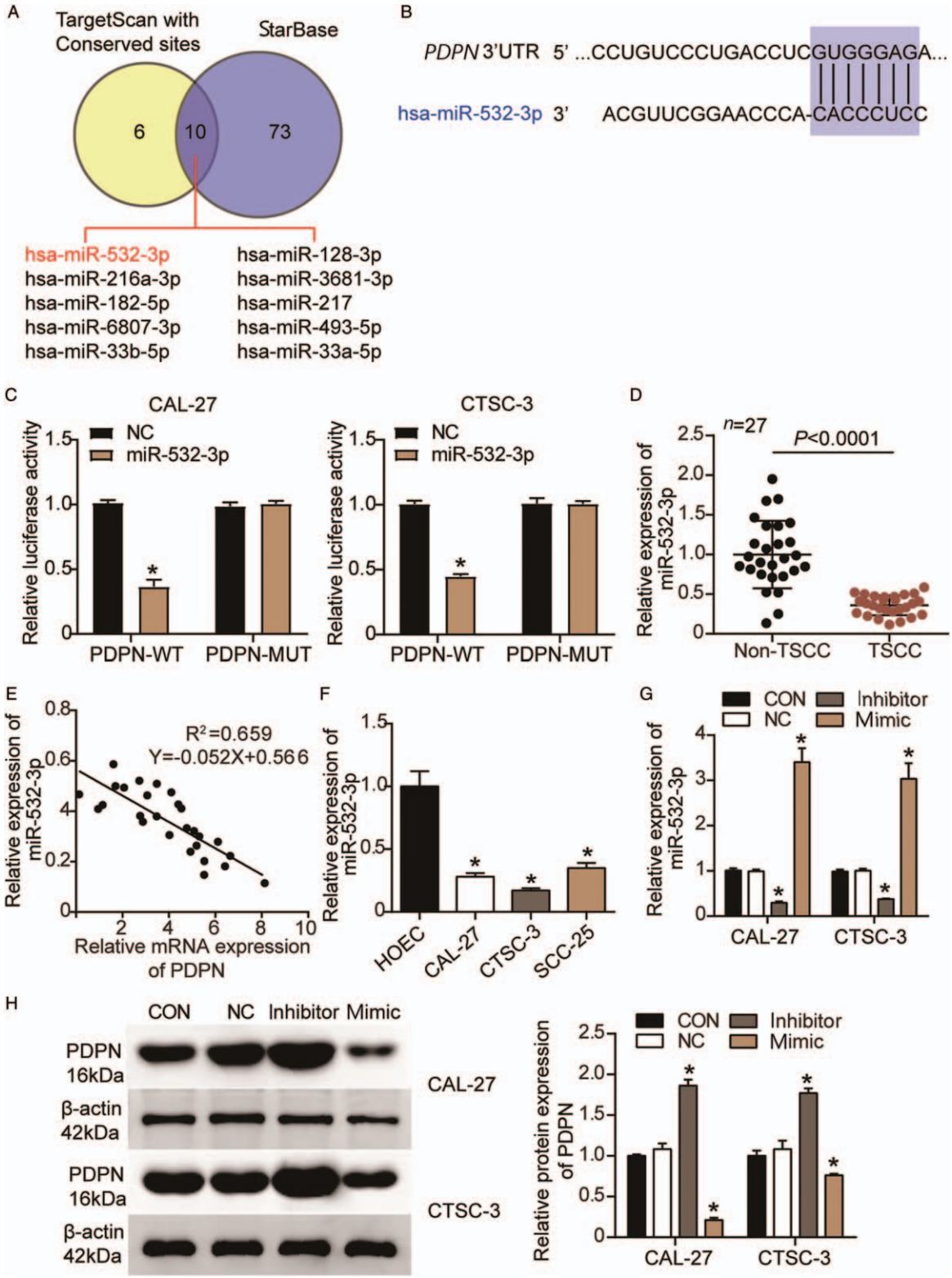

Figure 4: *PDPN* was identified as a target gene of miR-532-3p in TSCC cells. (A): Ten miRNAs targeting *PDPN* overlapped between TargetScan and starBase. (B): The predicted binding sites for miR-532-3p on the *PDPN* 3′UTR. (C): A DLR assay was performed to verify the binding of miR-532-3p to *PDPN*. WT: Wild-type; MUT: Mutant; NC: miR-532-3p mimic NC; $^{*}P < 0.001$ *vs.* the miR-532-3p mimic NC. (D): The relative expression of miR-532-3p in TSCC tissues and corresponding non-TSCC tissues as determined by RT-qPCR. (E): The correlation between miR-532-3p and *PDPN* in TSCC tissues was analyzed by Pearson's correlation. (F): The relative expression of miR-532-3p in the HOEC and TSCC cell lines (CAL-27, CTSC-3, and SCC-25) as determined by RT-qPCR. (G): The transfection efficiency of the miR-532-3p inhibitor and mimic in CAL-27 and CTSC-3 cells. $^{*}P < 0.001$ *vs.* the blank control group. (H): The protein expression of *PDPN* in CAL-27 and CTSC-3 cells after the transfection of the miR-532-3p inhibitor and mimic. CON: Blank control group; DLR: Dual-luciferase reporter; HOEC: Human normal oral epithelial cell; miRNAs: MicroRNAs; NC: Negative control; *PDPN*: Podoplanin; RT-qPCR: Quantitative real-time reverse transcription-polymerase chain reaction; TSCC: Tongue squamous cell carcinoma. $^{*}P < 0.001$ *vs.* the blank control group.

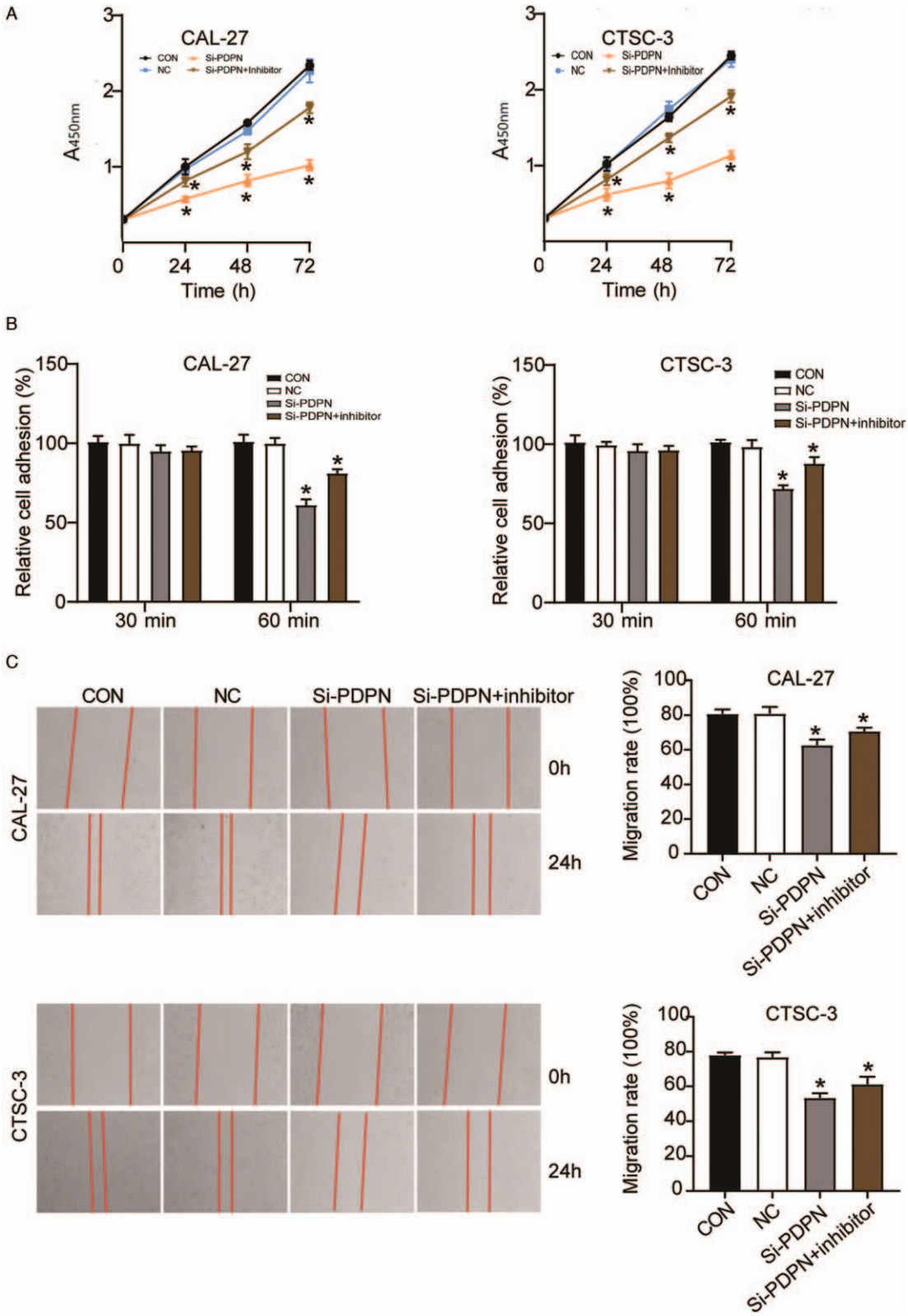

Figure 5: The miR-532-3p inhibitor could reverse the tumor inhibitory effect of *PDPN* knockdown. The cells were transfected with si-PDPN or si-PDPN plus the miR-532-3p inhibitor. (A) A CCK-8 assay was performed to detect the viability of CAL-27 and CTSC-3 cells. (B): A cell adhesion assay was performed to assess the adhesive ability of CAL-27 and CTSC-3 cells. (C) A wound-healing assay was performed to evaluate the migratory ability of CAL-27 and CTSC-3 cells. CCK-8: Cell counting kit-8; CON: Blank control group; NC: Negative control; *PDPN*: Podoplanin. $^{*}P < 0.05$ *vs.* the blank control group.

$P < 0.001$, respectively) was increased compared with that in the si-PDPN group (62.70 ± 3.29% and 53.40 ± 2.68%, respectively) [Figure 5C]. Collectively, the results demonstrated that miR-532-3p inhibitor treatment could reverse the tumor inhibitory effect of *PDPN* knockdown.

Discussion

In this study, we assessed the impacts of the miR-532-3p/*PDPN* axis on TSCC progression. First, we observed that *PDPN* expression was enriched in TSCC tissues and cells, and determined that *PDPN* could promote TSCC progression by enhancing the viability, adhesive capacity, and migratory capacity of TSCC cells. Additionally, we discovered that *PDPN* was a target of miR-532-3p and that *PDPN* expression could be inhibited by miR-532-3p in TSCC cells. Moreover, in TSCC cells, miR-532-3p inhibitor treatment could reverse the anti-tumor effect of *PDPN* knockdown.

The protein product of *PDPN* has been discovered to be closely associated with oral carcinomatosis. Studies have suggested that *PDPN* can serve as a biomarker for oral carcinogenesis and that *PDPN* overexpression in oral tissues can lead to malignant disorders and oral cancer.[28] Similarly, two studies reported that *PDPN* facilitated tumor development by promoting cell migration and invasion.[12,29] Oral squamous cell carcinomas are the most common type of oral cancer,[30] with TSCC being the most prevalent.[31] Although experimental data support the tumor-promoting role of *PDPN* in oral cancer, little is known about the roles played by *PDPN* in the progression of TSCC. In this research, we noticed that *PDPN* was significantly enriched in TSCC tissues and cells and that it played a stimulatory role in TSCC development, which was in agreement with the outcomes reported in the literature. Our findings also revealed the tumor-promoting role of *PDPN* in TSCC. Specifically, we found that by targeting *PDPN*, miR-532-3p inhibited the viability of TSCC cells, as well as their adhesive and migratory capacity (CAL-27 and CTSC-3 cells).

Several studies reported that abnormally expressed miRNAs participate in the progression of multiple cancer types, including breast cancer[32] and gastric cancer.[33] Specifically, miR-532-3p has been demonstrated to be highly expressed in tumor tissues and to promote cancer development. However, miR-532-3p has also been documented as playing a tumor-suppressor role in ovarian carcinoma,[34] non-small cell lung carcinoma,[35] lymphoma,[36] and colorectal carcinoma.[37] A recent study reported that miR-532-3p was sponged by circMDM2, thus suppressing the proliferation of oral squamous cell carcinoma. Another study focused on the function of miR-532-3p in TSCC and found that high miR-532-3p expression could suppress cell proliferation and enhance cell apoptosis in TSCC cell lines by targeting CCR7.[26] Our study demonstrated that by targeting *PDPN*, the miR-532-3p inhibitor reversed the suppressive effect of si-PDPN on CAL-27 and CTSC-3 cell viability, adhesion, and migration. Our results agree with those of previous studies even though we used different cellular materials, experimental methods, and downstream genes.

Although we demonstrated the impact of the miR-532-3p/*PDPN* axis on TSCC development, this study had several limitations. The effect of the miR-532-3p/*PDPN* axis on TSCC development involves a complex regulatory network, including signaling pathways. However, we did not explore this complexity, and future research should examine this aspect. Also, *in vivo* experiments were not conducted in this study due to limited funds. These limitations should be considered in future studies on TSCC.

Collectively, our results demonstrated that miR-532-3p plays a crucial role in TSCC progression by targeting *PDPN*. Furthermore, *PDPN* was observed to be significantly enriched in TSCC tissues, and could enhance the adhesive capacity, viability, and migratory ability of TSCC cells. However, the promotive effect of *PDPN* on TSCC cells could be relieved by miR-532-3p. These findings suggested that the miR-532-3p/*PDPN* axis might be a novel therapeutic target for the treatment of TSCC.

Conflicts of interest

None.

References

1. Sano D, Myers JN. Metastasis of squamous cell carcinoma of the oral tongue. Cancer Metastasis Rev 2007;26:645–662. doi: 10.1007/s10555-007-9082-y.
2. Zheng G, Zhang Z, Liu H, Xiong Y, Luo L, Jia X, *et al*. HSP27-mediated extracellular and intracellular signaling pathways synergistically confer chemoresistance in squamous cell carcinoma of tongue. Clin Cancer Res 2018;24:1163–1175. doi: 10.1158/1078-0432.CCR-17-2619.
3. Fan T, Pi H, Li M, Ren Z, He Z, Zhu F, *et al*. Inhibiting MT2-TFE3-dependent autophagy enhances melatonin-induced apoptosis in tongue squamous cell carcinoma. J Pineal Res 2018;64:e12457. doi: 10.1111/jpi.12457.
4. Enokida T, Fujii S, Takahashi M, Higuchi Y, Nomura S, Wakasugi T, *et al*. Gene expression profiling to predict recurrence of advanced squamous cell carcinoma of the tongue: discovery and external validation. Oncotarget 2017;8:61786–61799. doi: 10.18632/oncotarget.18692.
5. Mendenhall WM, Stringer SP, Amdur RJ, Hinerman RW, Moore-Higgs GJ, Cassisi NJ. Is radiation therapy a preferred alternative to surgery for squamous cell carcinoma of the base of tongue? J Clin Oncol 2000;18:35–42. doi: 10.1200/JCO.2000.18.1.35.
6. Hussein AA, Forouzanfar T, Bloemena E, de Visscher J, Brakenhoff RH, Leemans CR, *et al*. A review of the most promising biomarkers for early diagnosis and prognosis prediction of tongue squamous cell carcinoma. Br J Cancer 2018;119:724–736. doi: 10.1038/s41416-018-0233-4.
7. Chen Y, Tian T, Li ZY, Wang CY, Deng R, Deng WY, *et al*. FSCN1 is an effective marker of poor prognosis and a potential therapeutic target in human tongue squamous cell carcinoma. Cell Death Dis 2019;10:356. doi: 10.1038/s41419-019-1574-5.
8. Oki H, Kaneko MK, Ogasawara S, Tsujimoto Y, Liu X, Sugawara M, *et al*. Characterization of monoclonal antibody LpMab-7 recognizing non-PLAG domain of podoplanin. Monoclon Antib Immunodiagn Immunother 2015;34:174–180. doi: 10.1089/mab.2014.0090.
9. Agarwal D, Pardhe N, Bajpai M, Gupta S, Mathur N, Vanaki SS, *et al*. Characterization, localization and patterning of lymphatics and blood vessels in oral squamous cell carcinoma: A comparative study using D2-40 and CD-34 IHC marker. J Clin Diagn Res 2014;8:ZC86–ZC89. doi: 10.7860/JCDR/2014/10311.5072.
10. Hu L, Zhang P, Sun W, Zhou L, Chu Q, Chen Y. PDPN is a prognostic biomarker and correlated with immune infiltrating in gastric cancer. Medicine (Baltimore) 2020;99:e19957. doi: 10.1097/MD.0000000000019957.

11. Xie L, Lin C, Zhang Q, Piao H, Bigner DD, Zhang Z, *et al*. Elevated expression of podoplanin and its clinicopathological, prognostic, and therapeutic values in squamous non-small cell lung cancer. Cancer Manag Res 2018;10:1329–1340. doi: 10.2147/CMAR.S163510.
12. Retzbach EP, Sheehan SA, Nevel EM, Batra A, Phi T, Nguyen ATP, *et al*. Podoplanin emerges as a functionally relevant oral cancer biomarker and therapeutic target. Oral Oncol 2018;78:126–136. doi: 10.1016/j.oraloncology.2018.01.011.
13. de Vicente JC, Rodrigo JP, Rodriguez-Santamarta T, Lequerica-Fernández P, Allonca E, García-Pedrero JM. Podoplanin expression in oral leukoplakia: tumorigenic role. Oral Oncol 2013;49:598–603. doi: 10.1016/j.oraloncology.2013.02.008.
14. Ohta M, Abe A, Ohno F, Hasegawa Y, Tanaka H, Maseki S, *et al*. Positive and negative regulation of podoplanin expression by TGF-(and histone deacetylase inhibitors in oral and pharyngeal squamous cell carcinoma cell lines. Oral Oncol 2013;49:20–26. doi: 10.1016/j.oraloncology.2012.06.017.
15. Yuan P, Temam S, El-Naggar A, Zhou X, Liu DD, Lee JJ, *et al*. Overexpression of podoplanin in oral cancer and its association with poor clinical outcome. Cancer 2006;107:563–569. doi: 10.1002/cncr.22061.
16. Funayama A, Cheng J, Maruyama S, Yamazaki M, Kobayashi T, Syafriadi M, *et al*. Enhanced expression of podoplanin in oral carcinomas in situ and squamous cell carcinomas. Pathobiology 2011;78:171–180. doi: 10.1159/000324926.
17. Lee HY, Yu NY, Lee SH, Tsai HJ, Wu CC, Cheng JC, *et al*. Podoplanin promotes cancer-associated thrombosis and contributes to the unfavorable overall survival in an ectopic xenograft mouse model of oral cancer. Biomed J 2020;43:146–162. doi: 10.1016/j.bj.2019.07.001.
18. Bartel DP. MicroRNAs: genomics, biogenesis, mechanism, and function. Cell 2004;116:281–297. doi: 10.1016/s0092-8674(04)00045-5.
19. Hata A, Lieberman J. Dysregulation of microRNA biogenesis and gene silencing in cancer. Sci Signal 2015;8:re3. doi: 10.1126/scisignal.2005825.
20. Dragomir M, Mafra ACP, Dias SMG, Vasilescu C, Calin GA. Using microRNA networks to understand cancer. Int J Mol Sci 2018;19:1871. doi: 10.3390/ijms19071871.
21. Shi B, Yan W, Liu G, Guo Y. MicroRNA-488 inhibits tongue squamous carcinoma cell invasion and EMT by directly targeting ATF3. Cell Mol Biol Lett 2018;23:28. doi: 10.1186/s11658-018-0094-0.
22. Chen H, Dai J. miR-409-3p suppresses the proliferation, invasion and migration of tongue squamous cell carcinoma via targeting RDX. Oncol Lett 2018;16:543–551. doi: 10.3892/ol.2018.8687.
23. Wei T, Cong X, Wang XT, Xu XJ, Min SN, Ye P, *et al*. Interleukin-17A promotes tongue squamous cell carcinoma metastasis through activating miR-23b/versican pathway. Oncotarget 2017;8:6663–6680. doi: 10.18632/oncotarget.14255.
24. Chen D, Li J, Li S, Han P, Li N, Wang Y, *et al*. miR-184 promotes cell proliferation in tongue squamous cell carcinoma by targeting SOX7. Oncol Lett 2018;16:2221–2228. doi: 10.3892/ol.2018.8906.
25. Chen S, Zhang J, Sun L, Li X, Bai J, Zhang H, *et al*. miR-611 promotes the proliferation, migration and invasion of tongue squamous cell carcinoma cells by targeting FOXN3. Oral Dis 2019;25:1906–1918. doi: 10.1111/odi.13177.
26. Feng C, So HI, Yin S, Su X, Xu Q, Wang S, *et al*. MicroRNA-532-3p suppresses malignant behaviors of tongue squamous cell carcinoma via regulating CCR7. Front Pharmacol 2019;10:940. doi: 10.3389/fphar.2019.00940.
27. Amin MB, Greene FL, Edge SB, Compton CC, Gershenwald JE, Brookland RK, *et al*. The eighth edition AJCC cancer staging manual: continuing to build a bridge from a population-based to a more "personalized" approach to cancer staging. CA Cancer J Clin 2017;67:93–99. doi: 10.3322/caac.21388.
28. Swain N, Kumar SV, Routray S, Pathak J, Patel S. Podoplanin—A novel marker in oral carcinogenesis. Tumour Biol 2014;35:8407–8413. doi: 10.1007/s13277-014-2266-5.
29. Krishnan H, Rayes J, Miyashita T, Ishii G, Retzbach EP, Sheehan SA, *et al*. Podoplanin: an emerging cancer biomarker and therapeutic target. Cancer Sci 2018;109:1292–1299. doi: 10.1111/cas.13580.
30. Dumache R. Early diagnosis of oral squamous cell carcinoma by salivary microRNAs. Clin Lab 2017;63:1771–1776. doi: 10.7754/Clin.Lab.2017.170607.
31. Chen J, Liu L, Cai X, Yao Z, Huang J. Progress in the study of long noncoding RNA in tongue squamous cell carcinoma. Oral Surg Oral Med Oral Pathol Oral Radiol 2020;129:51–58. doi: 10.1016/j.oooo.2019.08.011.
32. Liu M, Luo C, Dong J, Guo J, Luo Q, Ye C, *et al*. CircRNA_103809 suppresses the proliferation and metastasis of breast cancer cells by sponging microRNA-532-3p (miR-532-3p). Front Genet 2020;11:485. doi: 10.3389/fgene.2020.00485.
33. Dai X, Liu J, Guo X, Cheng A, Deng X, Guo L, *et al*. Circular RNA circFGD4 suppresses gastric cancer progression via modulating miR-532-3p/APC/(-catenin signalling pathway. Clin Sci (Lond) 2020;134:1821–1839. doi: 10.1042/CS20191043.
34. Huang K, Fan WS, Fu XY, Li YL, Meng YG. Long noncoding RNA DARS-AS1 acts as an oncogene by targeting miR-532-3p in ovarian cancer. Eur Rev Med Pharmacol Sci 2019;23:2353–2359. doi: 10.26355/eurrev_201903_17379.
35. Jiang W, Zheng L, Yan Q, Chen L, Wang X. miR-532-3p inhibits metastasis and proliferation of non-small cell lung cancer by targeting FOXP3. J BUON 2019;24:2287–2293. https://www.jbuon.com/archive/24-6-2287.pdf.
36. Liu Y, Li Q, Dai Y, Jiang T, Zhou Y. miR-532-3p inhibits proliferation and promotes apoptosis of lymphoma cells by targeting (-catenin. J Cancer 2020;11:4762–4770. doi: 10.7150/jca.45684.
37. Gu C, Cai J, Xu Z, Zhou S, Ye L, Yan Q, *et al*. miR-532-3p suppresses colorectal cancer progression by disrupting the ETS1/TGM2 axis-mediated Wnt/β-catenin signaling. Cell Death Dis 2019;10:739. doi: 10.1038/s41419-019-1962-x.

How to cite this article: Liu ZY, Zhao CG. miR-532-3p inhibits the progression of tongue squamous cell carcinoma by targeting podoplanin. Chin Med J 2021;134:2999–3008. doi: 10.1097/CM9.0000000000001563